

# Generate and Verify Semantically Meaningful Formal Analysis of Neural Network Perception Systems

C. R. Serrano, P. M. Sylla, M. A. Warren

Information and Systems Sciences Laboratory  
HRL Laboratories LLC  
Malibu, CA

## Abstract

Testing remains the primary method to evaluate the accuracy of neural network perception systems. Prior work on the formal verification of neural network perception models has been limited to notions of local adversarial robustness for classification with respect to individual image inputs. In this work, we propose a notion of global correctness for neural network perception models performing regression with respect to a generative neural network with a semantically meaningful latent space. That is, against an infinite set of images produced by a generative model over an interval of its latent space, leverage neural network verification tools to prove that a perception model will always produce estimates within some error bound of the ground truth. Where the perception model fails these tools will return a semantically meaningful counter-example. These counter-examples are semantically meaningful in the sense that they carry information on concrete states of the system of interest that can be used programmatically without human inspection of corresponding generated images. Our approach, Generate and Verify, provides a new technique to gather insight into the failure cases of neural network perception systems and provide meaningful guarantees of correct behavior in safety critical applications.

## 1 Introduction

One would often like to know whether or not a neural network perception system produces correct estimates and, moreover, when it will fail to do so. The naïve approach to this question is to gather more data against which to evaluate system performance. This gives a necessarily incomplete picture: we can only ever evaluate a finite set of individual data points (e.g., images), and, in most cases, it will be impossible to meaningfully capture the totality of relevant data the system might encounter in its operational environment by such a set. Indeed,

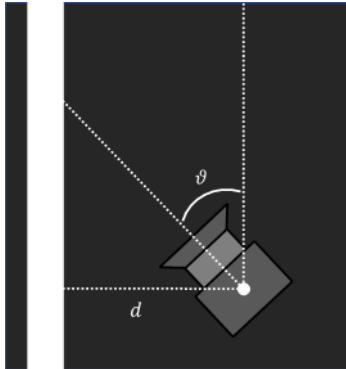


Figure 1: Example of configuration space for simple distance to line estimation. Here  $d$  is the distance in meters to the line and  $\theta$  is the yaw angle.

part of the appeal of neural networks and machine learning is their ability to, in many cases, successfully generalize to unseen data.

A recent alternative approach utilizes neural network verification tools built on techniques such as satisfiability modulo theories (SMT), mixed integer linear programming (MILP), or other techniques from logic and computational geometry to mathematically analyze the neural network and produce either proof artifacts, capturing mathematical guarantees on performance, or counter-examples, indicating cases where mathematical guarantees are impossible. Crucially, because of the analytical approach of neural network verification, the guarantees obtained are universally quantified and therefore apply to an entire region of the input space of the network encompassing infinitely many input values. The skeptical reader should compare this with cases such as linear programming, where (in infeasible instances) similar guarantees over infinite sets are possible. Neural network verification promises to powerfully complement testing, but it has primarily been leveraged in the perception domain in connection with *local adversarial robustness* properties of the form: *Given a model and fixed image  $x$ , does there exist a perturbation  $\delta$  bounded in norm below some fixed constant  $\epsilon > 0$  such that the perturbed image  $(x + \delta)$  is classified differently from  $x$  by the model?*

Beyond local adversarial robustness and related properties, such as invariance under specified transformations, the use of neural network verification to analyze perception systems is a challenge, due to the fact that most of the desirable properties of such systems cannot be formally specified. Having a formal, mathematically well-defined, specification is a prerequisite for the use of these techniques. E.g., how would one specify the property that a classifier will correctly classify pedestrians in a formal, and non-statistical/empirical, mathematical manner? It is apparent that the formal specification of such properties in a way that can be analyzed by neural network verification is impossible. Nonetheless, our goal in this paper is to show that, by the use of generative

models (which introduce an empirical/statistical component to the analysis), it is possible to use neural network verification techniques to specify and formally reason over more general model properties than local adversarial robustness and transformation invariance.

If we are interested in global correctness with respect to semantically meaningful specifications, then the images over which we reason will need to be drawn from a semantically meaningful latent space. Our approach to global correctness first defines a semantically meaningful *configuration space* capturing the properties of the scenario depicted in images of the kinds we wish to reason over. As a motivating example, our work has focused on the analysis of a perception system for estimating the distance to a lane marker from images produced by a front facing vehicle mounted camera. The configuration space consists of the vehicle’s distance to the line  $d$ , and yaw angle  $\theta$  with respect to the line, as depicted in Figure 1.

To then verify properties of a neural network perception system with respect to our configuration space we require a function (the *decoder*) mapping from configuration space to image space, which can then be composed *in-line* with our regression perception system (the *regressor*). The formal analysis using neural network verification then reasons over a semantically meaningful region of the configuration space, and the output to be checked for correctness is that of our regressor. Each interval in our configuration space, assuming it is not degenerate, represents an infinite set of images against which the perception system will be verified for correctness.

Our approach, *Generate and Verify*, learns a neural network decoder from configuration space to image space against which the regressor can be verified. Our notion of global correctness is thus modulo the learned decoder. In the event the neural network verification cannot prove correctness it will generally return a counter-example in configuration space, which can then be provided to the decoder to yield the exact image on which our perception system fails. In practice, we divide the set of intervals over our configuration space into smaller boxes so that we may parallelize computation, gather diverse counterexamples, and identify smaller regions over which our regressor may be provably correct. Our approach yields proof artifacts (certificates), and provides a method to find counter-examples, that traditional sample and test techniques cannot provide.

## 2 Related Works

Our work is closely related to prior work on the verification of neural networks [11, 12, 21, 22, 3, 18, 17, 20, 1, 2]. The setting for the tools developed in those works is as follows. Assume given an input set  $X$  (e.g. image space) and an output set  $Y$  where elements of  $Y$  correspond to either different discrete classes or probability vectors over classes. The neural network itself is mathematically regarded as a function  $f: X \rightarrow Y$  and the local robustness properties considered in the works above state that, for a fixed  $\epsilon > 0$  and input  $x$ , there exists no perturbation  $\delta$  with  $\|\delta\| < \epsilon$  (in a fixed norm, usually  $L_\infty$ ) such that  $f(x)$  and

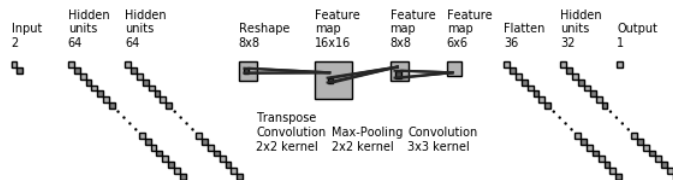


Figure 2: The combined decoder and regressor architecture. The decoder maps  $C$  space input to the  $16 \times 16$  intermediary image space  $I$  while the regressor maps from  $I$  to a single output  $\in \mathbb{R}$ .

$f(x + \delta)$  are too far from one another. Minor variations on this setting, where  $f(x + \delta)$  should not be too far from the true class, are also considered. This is a reasonable property to consider that directly relates to the phenomena of adversarial examples, but it tells us nothing about the kinds of images more generally on which the neural network will be likely to correctly perform. Instead, it merely bounds how far small perturbations  $\delta$  of *fixed images* are able to push the resulting output of the network.

A notable exception to the literature above is the technical report [4] in which an approach to global correctness obtained by pre-composing a generative model with an image classifier to find counter-examples through random search is described. Crucially, this work relies on the sampling of noise from a (semantically meaningless) latent space (of noise) to generate *finite* sets of images against which a classifier is tested. By contrast, our work first constructs a semantically meaningful space from which images are generated, and evaluates model correctness, using neural network verification, against *infinite* sets of images.

A final paper that is relevant to our work, but rather distinct, is [5] which introduces a formal language for specifying scenes and a compiler for rendering scenes in a pre-existing simulator. This approach has been used in conjunction with targeted testing of neural network vision systems. However, as with traditional testing, the outputs of this approach are the same as traditional sample and test approaches: individual instances of failure or success independent of any global correctness guarantee.

## 3 Background

### 3.1 Neural Network Verification

Our approach is largely agnostic regarding the choice of neural network verification tool: as long as the tool is capable of reasoning over the decoder and regressor it can be used. In the experiments described below, we used the general purpose *dReal* SMT solver [7]. The advantage of *dReal* is that, by virtue of the so-called “ $\delta$ -decidability theorem” of [6], *dReal* is able to handle reason-

ing over properties involving non-linear real arithmetic and all of the common non-linear functions (including transcendental functions). At a very high level, dReal transforms problems of real arithmetic with non-linear functions into the domain of interval analysis and then carries out a DPLL-style [8] branch-and-prune search by splitting boxes until a fixed precision (the “ $\delta$ ”) has been reached. Consequently, we are able to reason over neural networks with all common neural network architecture features: convolutions, transposed convolutions, ReLU, tanh, sigmoid, softmax, batch normalization, etc., can all be represented and reasoned over in dReal. In addition to dReal itself, we make use of a custom C++ library for transforming neural network models into a format that dReal can handle (dReal was designed to reason over scalars and our library can be regarded as a wrapper on dReal at the level of tensors).

In terms of usage, dReal is provided with a list of variables  $x_1, \dots, x_n$  over which we intend to solve. We provide also a property  $\varphi(x_1, \dots, x_n)$  to be evaluated. The results of the evaluation are of three kinds. First, when the property is satisfiable (*SAT*) dReal will provide us with a list  $a_1, \dots, a_n$  of concrete values such that  $\varphi(a_1, \dots, a_n)$  holds. When the property is unsatisfiable (*UNSAT*) dReal provides us with a mathematical proof (certificate) establishing that the property holds for non values of  $x_1, \dots, x_n$ . Finally, the property could be *unknown* in which dReal can be re-run with a smaller precision parameter  $\delta$ , although, due to undecidability of first-order real arithmetic with transcendental functions, we cannot guarantee that the process of progressively decreasing the magnitude of  $\delta$  and re-running dReal will result in a SAT or UNSAT.

The principal bottleneck to the broad use of neural network verification tools is scalability, although recent advances such as [21] are promising. With this in mind, we describe timing data on the use of the verification tools in detail below. It is worth noting that one advantage of our approach is that it moves the problem of neural network verification from high-dimensional image space, where these tools scale more poorly, to the lower dimensional spaces  $C$  and  $C \times Z$ , where these tools scale better.

### 3.2 Conditional Variational Auto-Encoder

A Conditional Variational Auto-Encoder [13] maximizes the variational lower bound of the data point  $x$  conditioned on variable  $c$ . During training, the data point  $x$  and its label  $c$  are provided as input to a conditional encoder  $q$  that maps the input to a noise latent space  $Z$ . Concretely, the conditional encoder learns a mapping from inputs  $(x, c)$  to a distribution  $Z$  parameterized by  $\mu$  and diagonal covariance matrix  $\Sigma$ . During training the encoder output  $z$  is then reparameterized with noise variable  $\epsilon$ ,  $\tilde{z} = z + \epsilon$ , via the *reparameterization trick* [13], and finally  $(z, c)$  is provided to the decoder  $p$  which maps back to image space  $I$ . The lower bound  $\tilde{\mathcal{L}}_{CVAE}(x, c; \varphi, \phi)$  is thus empirically defined as the sum

$$-KL(q_\phi(z|x, c)||p_\varphi(z|x)) + \frac{1}{N} \sum_{n=1}^N \log p_\varphi(c|x, z).$$

## 4 Generate and Verify

The configuration space  $C$  is a model of semantically meaningful features of the operational scenario that should be sufficient to evaluate the correctness of the system, thus  $\dim C$  corresponds to the number of such features. For example, in the case of estimation of the distance  $d$  from the camera to a lane marker on a road from image data produced by a front-mounted vehicle camera, assuming fixed camera pitch and roll angles, the configuration space could be the cylinder  $S^1 \times [-r, r]$  where  $r$  is an estimate of visual range. Here a point  $(\vartheta, d)$  in  $C$  corresponds to the physical scenario in which the camera is at a distance of  $d$  meters from the line oriented with a yaw angle of  $\vartheta$  radians with respect to the line, as depicted in Figure 1.

Given a set of images labeled with the ground truth in our configuration space, which may be gathered either from the real world or in simulation, our approach is to learn a deterministic decoder from configuration space to image space. The decoder may take the form of a traditional neural network decoder, as in the latter half of an autoencoder [10], or as a conditional generative model [19]. A conditional generative model allows us to condition our decoder on both our semantically meaningful configuration space  $C$  and a learned noise latent space  $Z$  to capture variation in the image distribution we either do not know how to, or do not wish to, define semantically. The input space to be solved over then becomes  $C \times Z$ .

---

### Algorithm 1: GENERATE AND VERIFY

---

**Data:** Target Task Model to be Verified  $P_\varphi$ , images  $X$  labeled with configuration  $c$ , reconstruction cost function  $\mathcal{L}$ , partition  $(B_i)$  of  $C$ , correctness properties  $\tau_i$  with universal quantifiers restricted to the corresponding cells  $B_i$ , Neural Network Verification Tool (Solver)  $\omega$ .

- 1 Initialize decoder  $G_\psi$  with random weights  $\psi$
- 2 **for** *epoch*  $e \in \{1, \dots, E\}$  **do**
- 3     sample random minibatch of training tuples  $(x, c)$
- 4      $\hat{x} = G_\psi(c)$
- 5     Perform a gradient descent step on  $\mathcal{L}(x, \hat{x})$ .
- 6 **for** *cell*  $i \in P$  **do**
- 7     return  $\omega(\tau_i, G_\psi, P_\varphi)$

---

In what follows, we denote by  $P_\varphi$  accepting input from image space  $I$  parameterized by  $\varphi$  and let  $G_\psi$  denote a neural network decoder mapping input from configuration space  $C$  to image space  $I$  parameterized by  $\psi$ . Let  $L$  denote a subset of  $C$ , then *global correctness modulo the decoder* is the following statement:

$$\forall c \in C. d(P_\varphi(G_\psi(c)), y) < \epsilon \tag{1}$$

In practice, we carry out the analysis separately over the individual cells of a *partition* of  $C$  as a union of cartesian products of closed intervals:

$$C \times Z = \bigcup_i \prod_j [b_{i,j}, u_{i,j}]$$

Each constituent cartesian product  $B_i := \prod_j [b_{i,j}, u_{i,j}]$  is referred to as a *cell* of the partition. We typically require cells to be almost mutually disjoint in the sense that  $B_i^\circ \cap B_k^\circ = \emptyset$  for  $i \neq k$ , where  $B_i^\circ$  denotes the interior of the set  $B_i$ .

Our algorithm operates in three stages: initialization, training, and solving. At the initialization stage, the user specifies a configuration space  $C$ , or  $C \times Z$ , as a list of variables together with their intended ranges.

Training the decoder is a standard supervised learning task utilizing labeled perception data  $X$  (e.g., images) such that the labels correspond to points in  $C$ . In the case of a conditional decoder, that is a decoder conditioned on  $C$  with learned noise latent  $Z$ , the training follows the standard conditional variational auto-encoder paradigm as previously outlined above (in Section Conditional Variational Auto-Encoder).

During analysis, a partition, and descriptions of the decoder and regressor neural network architectures, and their respective weights, are provided as inputs to our dReal-based neural network analysis tool summarized in (Section Neural Network Verification above). For each cell of the partition the analysis outputs one of the following:

1. a mathematical proof of correctness;
2. a counter-example indicating the presence of a failure case in the cell; or
3. an indication that nothing could be determined regarding the cell.

Here the notion of correctness corresponds to (1), but with the universal quantification restricted to the individual cells  $B_i$ . The parameters required are the constant  $\varepsilon$  from (1) and the precision  $\delta$  used by dReal.

The aggregation of analysis returns over the partition is called a *proof map*. In the case of a two-dimensional proof map (as is the case in our first experiment) it can be visualized as a heat map, as seen in Figure 5. Mathematically, a proof map is a map  $m : I \rightarrow \{-1, 0, 1\}$  where  $I$  is the index set of the partition. Intuitively,  $m(i) = 1$  indicates that there exists a configuration in cell  $B_i$  that causes the target model to produce an incorrect estimate. Similarly,  $m(i) = -1$  indicates that the tool was able to generate a mathematical proof that, relative to inputs to the target model generated by the decoder, the target model produces correct estimates for all configurations in cell  $B_i$ . Finally,  $m(i) = 0$  indicates that the tool was unable to produce a mathematical proof of correctness for, or to find an example where an incorrect estimate is produced by a configuration, in cell  $B_i$ . In order to speed up proof map generation some sampling can be carried out in order to rule out some cells with  $m(i) = 1$  prior to handing the analysis over to dReal. In our experiments, we merely pre-processed by evaluating the centers of cells, but more nuanced schemes could be deployed.

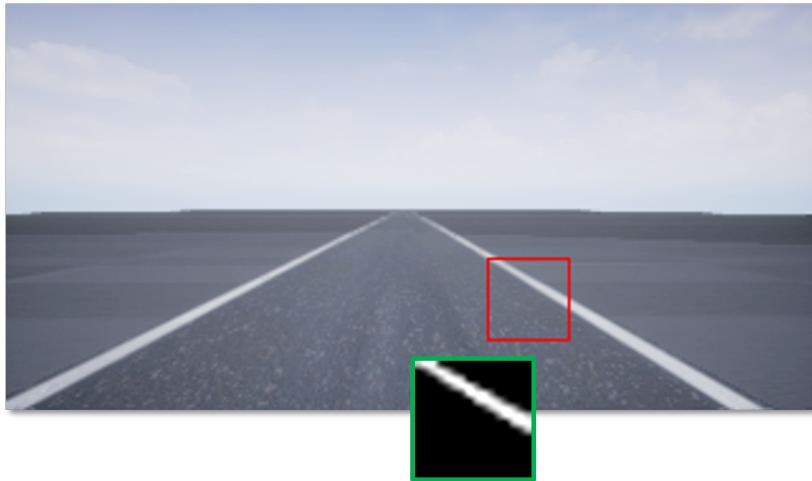


Figure 3: Original camera image from the AirSim simulation environment. Crop outlined in red, post processed training image inset and outlined in green. View is from the point in configuration space ( $d = 1.5481, \theta = 0.0136$ ).

## 5 Experiments

We will describe our application of the Generate and Verify approach to a neural network perception system performing regression in two experiments. In both experiments the task is to estimate the distance to a lane marker given an image from the front mounted camera of a vehicle. In the first experiment the configuration space consists only of two features: the distance in meters to the lane marker  $d$ , and the yaw angle of the vehicle  $\theta$ . A depiction of the configuration space can be seen in Figure 1. The roll and pitch are held fixed. In the second experiment an augmentation is randomly applied to each training image yielding a break in the line of variable width. This augmentation is not defined in the configuration space  $C$ . Instead, it is captured by a traditional Conditional Variational Auto-Encoder as a learned feature in a latent space  $Z$ .

The training images are collected in the AirSim [16] autonomous driving simulator in a single lane training environment. After capture, an image is converted to grayscale, a square crop of the image is taken at a fixed point in the frame, and the resulting crop is thresholded to yield a black and white image. Finally the cropped image is resized to  $16 \times 16$  pixels. The preprocessing pipeline is depicted in Figure 3. 10,000 such images are collected in simulation, along with their  $C$  space ground truth labels, to construct the decoder training set  $X$ . The structural similarity index measure (SSIM) between the original images  $X$  and their decoder reconstructions  $\hat{X}$  was measured to be 0.823. Representative images  $x$  and both their decoder and conditional decoder reconstructions  $\hat{x}$  from six points in  $C$  space are presented in Figure 4.

Metrics for the evaluation of generative image models are an active area of





Figure 4: A set of six training images (top), their reconstructions (middle), and reconstructions conditioned on  $z = 0$  (bottom) from six different points in configuration space.

research and recently the Fréchet Inception Distance (FID) [9] and Improved Precision and Recall (P&R) [14] have gained in popularity in the GAN literature. FID measures the Wasserstein-2 distance between two multidimensional Gaussians defined by the mean and covariance of the feature activations of an InceptionV3 classification model for the training images and generated images, respectively. P&R measures average sample quality (“precision”) of generated images and the sample distribution coverage (“recall”). While this work has not incorporated these metrics the generation of realistic images and associated metrics are actively studied and future applications of our method will benefit from advances in this research.

In the first experiment  $C$  fully describes the configuration space and the task of training the decoder is a simple supervised learning task with input configuration  $c$  being mapped to image output  $x$ . The network architecture consists of a 2D input and two 64 node dense hidden layers with ReLU activation. Finally, a 2D transposed convolution with a single input and output channel, kernel size  $2 \times 2$ , and stride 2, with sigmoid activation effectively upsamples the output of the final dense layer to yield a  $16 \times 16$  grayscale image. During training the weights of the decoder are updated such that they minimize the Binary Cross-Entropy loss between the ground truth image and the grayscale reconstruction.

The regressor perception network is trained independently on the same training data as was collected for the decoder. In the first experiment the regressor architecture consists of a  $16 \times 16$  pixel single channel image input, followed by an average pooling downsampling layer with kernel size  $2 \times 2$ , and stride 2. The pooling layer is followed by a single dense layer of 64 nodes with hyperbolic tangent activation and a single linear output. The hyperparameters used during training for both the decoder and regressor are summarized in Table 5.

In the first experiment analysis, we only considered  $C = [-3, -0.37] \times [-0.03, 0.17]$  and the partition a linearly spaced  $20 \times 20$  grid with a total of

400 cells. In this case, the precise definition of correctness states that the estimates are not too far from the ground-truth distance in the sense that:

$$\forall(d, \vartheta) \in B_i. \|P_\varphi(G_\psi(d, \vartheta)) - d\| < \epsilon$$

where the precision constant  $\epsilon$  is 0.25 and  $\|\cdot\|$  denotes the  $L_2$  norm.

In the second experiment, we consider  $C = [-1., -0.75] \times [-0.25, 0.2]$  and  $Z = [-0.1, 0.1]$  with a linear partition of size two along the  $Z$  axis and a linearly spaced  $11 \times 11$  grid along  $C$ . We also evaluated separately the same grid over  $C$  with the latent  $Z$  region  $[0.2, 0.3]$ . In this experiment we used  $\epsilon = 0.5$ .

## 5.1 Decoder Results

Figure 5 shows the proof map corresponding to our first experiment resulting from solving over the portion of  $C$  space with distance  $d \in [-3, 0]$  (negative values correspond to being left of the lane marker) and yaw angle  $\theta \in [-.1, .2]$ . The property proved is that the regressor will produce estimates for each point  $c$  within .25m of the ground truth. Counter-examples are found when the vehicle is near the lane marker at negative yaw values, and when distant from the lane marker (near 3 meters) at positive yaw angles. The regressor is found to be provably correct over 55% of the cells of the partition, with each cell  $b_i$  representing the infinite set of images the decoder could generate from the infinite set of points  $c$  within each cell. Crucially, the correct cells are not an approximation of the regressor’s accuracy with respect to the decoder in those regions of  $C$  space, as one would acquire with traditional sample and test techniques, rather they are regions in which the solver returns a mathematical proof that the regressor will return estimates within .25m of ground truth  $\forall c \in B_i$ . Summary statistics are provided in 3.

The total time taken to solve over the proof map partition in 5 was 208.43 hours, approximately 8.5 days. Each cell is solved by a separate process and a maximum of five cells are solved simultaneously. A heatmap of the time taken for each cell to return a result is visualized in Figure 5. It is apparent that counter-examples are returned more quickly than proofs of correctness. Further timing statistics and details regarding the machines on which our experiments were carried out are included in the appendix.

Hyperparameter	Value
batch size	64
optimizer	Adam
Learning rate	1e-4
Weight decay	5e-4
epochs	500,000

Table 1: Decoder and Regressor hyperparameters used during training.

## 5.2 Conditional Decoder Results

In the second experiment with equal probability a diagonal mask is applied to each training image yielding a break in the line of variable width, thus capturing the notion of one way in which our lane marker may be degraded in the real world. The configuration space  $C$  is identical to the first experiment, but we now concatenate it with the learned latent feature space  $Z$ .  $Z$ , and the decoder, are learned simultaneously in a CVAE architecture. The CVAE network architecture consists of encoder network  $q$  with input layer dimension  $(16 \times 16) + \dim C$ , followed by densely connected layers with ReLU activation of 8 nodes and 2 nodes respectively, and finally single linear outputs for each of the  $\mu$  and  $\sigma$  parameters of the latent space  $Z$ . The decoder architecture remained unaltered from the first experiment.

It should be noted that in order to maintain independence between the information in  $C$  and  $Z$ , that is, in order for the decoder output to remain fixed at a point  $c$  while  $z$  is varied, it was found that the capacity of the encoder needed to be limited. Now, by simply varying the values of our input  $z$  we can generate images of the entire range of lane marker degradation our learned model has captured, conditioned on our fixed point in  $C$  space.

The architecture of the regressor from the first experiment was found to be insufficient to handle the noise present in the images of the second experiment so a revised architecture was developed. The regressor in the second experiment consists of  $16 \times 16$  pixel single channel image input layer, followed by an average pooling layer with kernel size  $2 \times 2$  and stride 2. The downsampling pooling layer is followed by a 2D convolutional layer with single channel input and output, kernel size  $3 \times 3$ , stride of 1, no padding, and hyperbolic tangent activation. A dense layer of 32 nodes with hyperbolic tangent activation follows the convolutional layer before a final single output node with sigmoid activation provides scaled estimates of the distance  $d$ .

Proof maps, for latent regions  $[-0.1, 0]$  and  $[0, 0.1]$ , and timing heatmaps can be found in Figure 6. The result statistics are in Table 4.

## 6 Conclusion

We have described a novel approach to neural network evaluation that allows a more fine-grained analysis than state-of-the-art testing and simulation approaches: it allows us to, via mathematical analysis, survey an infinite set of

Network	Loss
Decoder	BCE
Conditional Decoder (CVAE)	BCE + KL Divergence
Regressor	Mean Squared Error

Table 2: Decoder and Regressor loss functions used during training.

Cell Result	Count	Percent
UNSAT	218	55%
SAT	56	14%
Unknown	126	32%

Table 3: Aggregated  $C$  space cell results.

Cell Result	Count	Percent
UNSAT	89	37%
SAT	88	36%
Unknown	65	27%

Table 4: Aggregated  $C \times Z$  space cell results.

possible scenarios/images, whereas testing/simulation necessarily only examines a finite set of such scenarios/images. Our approach complements that of traditional sample and test methods by allowing stronger assurance guarantees over infinite (non-measure zero) sets of images and active counter-example search, counter-examples that might otherwise only be found in production as *edge cases*. These counter-examples are particularly valuable in debugging and developing insight into our models and data as they tell us under exactly what inputs our model will fail. These counterexamples can lead us to the discovery of deficiencies in our training data and patterns of success and failure that may be attributable to strengths and defects in our model design. Our generative decoder can be further utilized to generate training data around failure cases, allowing us to both find and resolve so called edge case failures before ever encountering them through traditional testing or in production. Our training data was captured at a fixed camera rotation step size and our simple decoder is able to smoothly interpolate between view angles to generate correct intermediate views absent from the training data, and to correctly capture the relationship between camera distance and angle to the lane marker. These novel views are not captured in the dataset, and thus could not be tested against with traditional testing schemes. Further, we can capture additional data variation, and generate images with that variation that were not present in the data: our CVAE is able to generate images with a "line break" augmentation in a smooth range of no break, and narrow to wide break, from every viewing angle, despite seeing only a finite set of training data that did not capture this full variation. As we refine our models in production, our approach provides a way to verify that we have not introduced new failure cases into previously correct task performance [15]. Additionally, there are several important differences between our approach and state-of-the-art approaches in the verification of neural networks. In the literature on verification of neural networks the focus is always on local properties, in the sense described previously, and in particular on adversarial robustness properties (i.e., that the system will not behave differently when inputs are subject to small perturbations/disturbances). We address global notions of

correctness similar to those from [4], but where our notion is modulo a generative model with input space that has a semantically meaningful factor. This approach can help to answer questions of the form: are there physical configurations of objects that will give rise to incorrect estimates by the system. This link between the actual physical configuration and perception network correctness is entirely broken in the existing work on verification of neural networks. Our contribution is thus a novel perspective on the verification of correct behavior in neural network perception systems.

The principal drawback of our approach is the fact that current neural network verification tools scale poorly to large networks or apply only to those networks having prescribed architecture features. This limits the size of both the models we can analyze and the generative models that we can employ in the analysis. Nonetheless, we believe that future advances will make this approach increasingly tractable in general. In the mean time, our approach can furthermore be used to augment testing and adversarial machine learning based approaches to neural network robustness analysis.

## 7 Acknowledgments

We would like to thank Doug Stuart, Ramesh S., Huafeng Yu, Sicun Gao, and Aleksey Nogin for useful conversations on topics related to this paper. We are also grateful to Cem Saraydar, Tom Bui, Chad McFarland, Bala Chidambaram, Roy Matic, Mike Daily and Son Dao for their support of and guidance regarding this research.

## A Machine Information and Hyperparameter Tables

The machine learning experiments were carried out on a machine with Intel Xeon E5-2680 v4 @ 2.40GHz processor and two NVIDIA Tesla P100-SXM2-16GB GPUs. The neural network verification was done on a machine with Intel Xeon E5-2690 v3 at 2.60GHz processor, 24 CPU cores, and 1TB of memory.

<b>Hyperparameter</b>	<b>Value</b>
batch size	64
optimizer	Adam
Learning rate	1e-4
Weight decay	5e-4
epochs	500,000

Table 5: Decoder and Regressor hyperparameters used during training.

Network	Loss
Decoder	Binary Cross Entropy (BCE)
Conditional Decoder (CVAE)	BCE + KL Divergence
Regressor	Mean Squared Error

Table 6: Decoder and Regressor loss functions used during training.

## References

- [1] Mislav Balunovic, Maximilian Baader, Gagandeep Singh, Timon Gehr, and Martin T. Vechev. Certifying geometric robustness of neural networks. In *NeurIPS*, 2019.
- [2] Elena Botoeva, Panagiotis Kouvaros, Jan Kronqvist, Alessio Lomuscio, and Ruth Misener. Efficient verification of relu-based neural networks via dependency analysis. In *AAAI*, 2020.
- [3] S. Dutta, Taisa Kushner, Susmit Jha, S. Sankaranarayanan, N. Shankar, and A. Tiwari. Sherlock : A tool for verification of deep neural networks. 2019.
- [4] Nathanael Fijalkow and M. Gupta. Verification of neural networks: Specifying global robustness using generative models. *ArXiv*, abs/1910.05018, 2019.
- [5] Daniel J. Fremont, T. Dreossi, S. Ghosh, Xiangyu Yue, A. Sangiovanni-Vincentelli, and S. Seshia. Scenic: a language for scenario specification and scene generation. *Proceedings of the 40th ACM SIGPLAN Conference on Programming Language Design and Implementation*, 2019.
- [6] S. Gao, J. Avigad, and E. M. Clarke. Delta-decidability over the reals. In *Proceedings of the 27th Annual ACM/IEEE Symposium on Logic in Computer Science (LICS)*, 2012.
- [7] Sicun Gao, Soonho Kong, and Edmund M Clarke. dreal: An smt solver for nonlinear theories over the reals. In *International conference on automated deduction*, pages 208–214. Springer, 2013.
- [8] Carla P. Gomes, Henry A. Kautz, Ashish Sabharwal, and Bart Selman. Satisfiability solvers. In Frank van Harmelen, Vladimir Lifschitz, and Bruce W. Porter, editors, *Handbook of Knowledge Representation*, volume 3 of *Foundations of Artificial Intelligence*, pages 89–134. Elsevier, 2008.
- [9] Martin Heusel, Hubert Ramsauer, Thomas Unterthiner, Bernhard Nessler, and Sepp Hochreiter. Gans trained by a two time-scale update rule converge to a local nash equilibrium. In *Advances in neural information processing systems*, pages 6626–6637, 2017.

- [10] Geoffrey E. Hinton and R. Salakhutdinov. Reducing the dimensionality of data with neural networks. *Science*, 313:504 – 507, 2006.
- [11] G. Katz, C. Barrett, D. Dill, Kyle Julian, and Mykel J. Kochenderfer. Reluplex: An efficient smt solver for verifying deep neural networks. In *CAV*, 2017.
- [12] G. Katz, Derek A. Huang, D. Ibeling, Kyle Julian, C. Lazarus, R. Lim, Parth Shah, Shantanu Thakoor, Haoze Wu, Aleksandar Zeljic, D. Dill, Mykel J. Kochenderfer, and C. Barrett. The marabou framework for verification and analysis of deep neural networks. In *CAV*, 2019.
- [13] Diederik P Kingma and Max Welling. Auto-encoding variational bayes. *arXiv preprint arXiv:1312.6114*, 2013.
- [14] Tuomas Kynkäänniemi, Tero Karras, Samuli Laine, Jaakko Lehtinen, and Timo Aila. Improved precision and recall metric for assessing generative models. In *Advances in Neural Information Processing Systems*, pages 3927–3936, 2019.
- [15] Michael McCloskey and Neal J Cohen. Catastrophic interference in connectionist networks: The sequential learning problem. In *Psychology of learning and motivation*, volume 24, pages 109–165. Elsevier, 1989.
- [16] Shital Shah, Debadeepta Dey, Chris Lovett, and Ashish Kapoor. Airsim: High-fidelity visual and physical simulation for autonomous vehicles. In *FSR*, 2017.
- [17] Gagandeep Singh, Rupanshu Ganvir, Markus Püschel, and Martin T. Vechev. Beyond the single neuron convex barrier for neural network certification. In *NeurIPS*, 2019.
- [18] Gagandeep Singh, Timon Gehr, Markus Püschel, and Martin T. Vechev. An abstract domain for certifying neural networks. *Proceedings of the ACM on Programming Languages*, 3:1 – 30, 2019.
- [19] Kihyuk Sohn, Honglak Lee, and Xinchen Yan. Learning structured output representation using deep conditional generative models. In *NIPS*, 2015.
- [20] Vincent Tjeng, K. Xiao, and Russ Tedrake. Evaluating robustness of neural networks with mixed integer programming. In *ICLR*, 2019.
- [21] H. Tran, Stanley Bak, W. Xiang, and Taylor T. Johnson. Verification of deep convolutional neural networks using imagestars. *Computer Aided Verification*, 12224:18 – 42, 2020.
- [22] H. Tran, Diego Manzananas Lopez, Patrick Musau, Xiaodong Yang, L. V. Nguyen, W. Xiang, and Taylor T. Johnson. Star-based reachability analysis of deep neural networks. In *FM*, 2019.

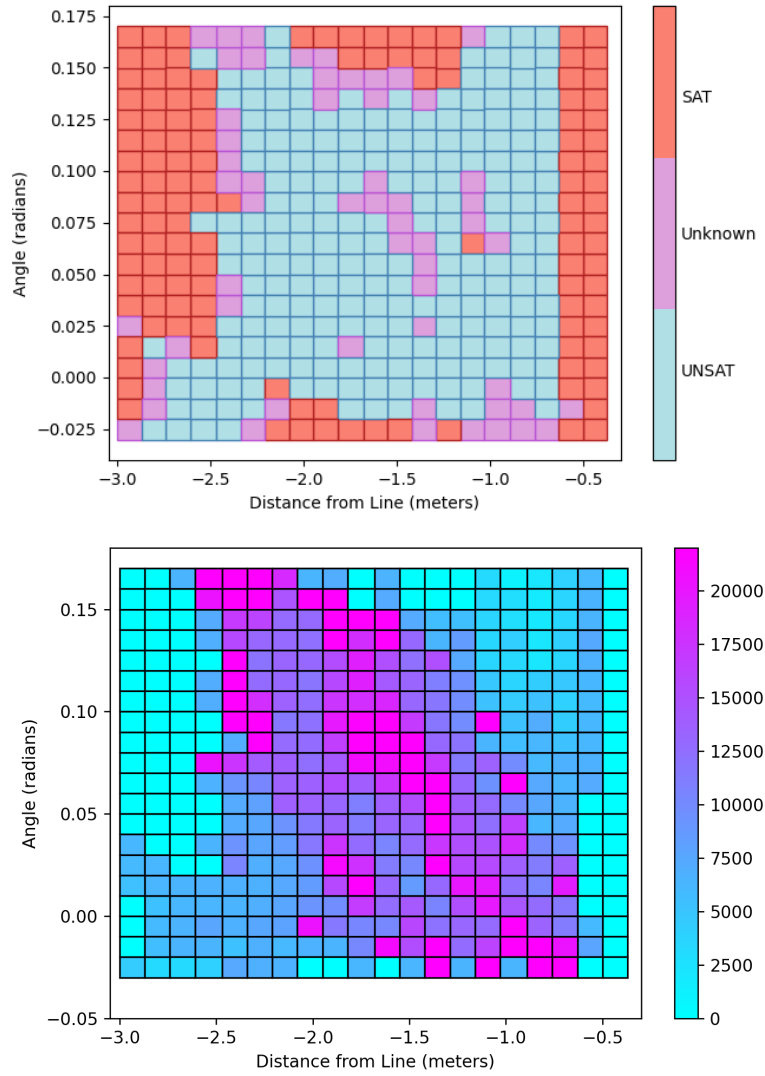


Figure 5: Proof map (left) over  $C$  space when  $\epsilon = 0.25$ . SAT (red) cells contain counterexamples, Unknown (purple) cells are inconclusive, and UNSAT (blue) cells are provably correct over the infinite set of states contained in the interval of state space they represent. Heatmap (right) of cell solving times in seconds.



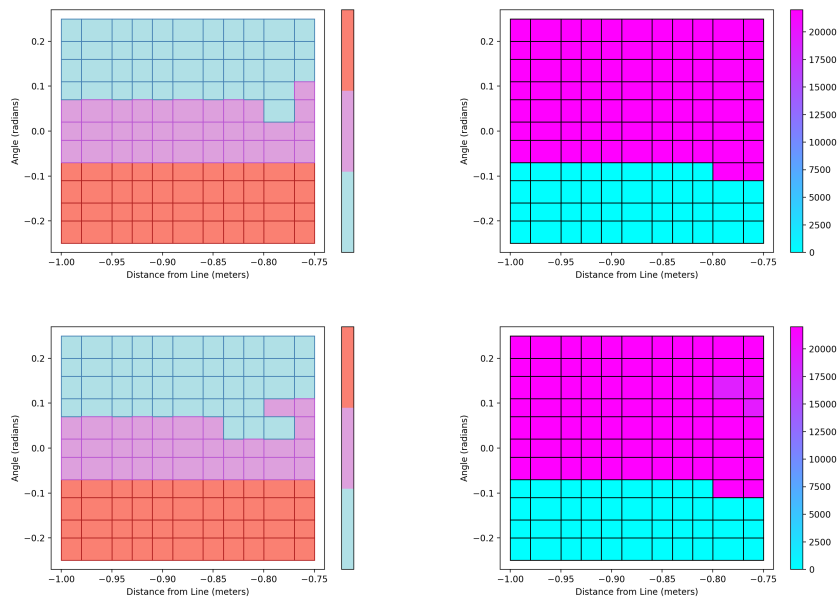


Figure 6: Proof map over  $C \times Z$  space when  $\epsilon = 0.5$  in the latent regions  $-0.1 \leq z \leq 0.0$  (top left) and  $0.0 \leq z \leq 0.1$  (bottom left). SAT (red) cells contain counterexamples, Unknown (purple) cells are inconclusive, and UNSAT (blue) cells are provably correct over the infinite set of states contained in the interval of state space they represent. Heatmaps (right) of cell solving times in seconds for the same latent regions.

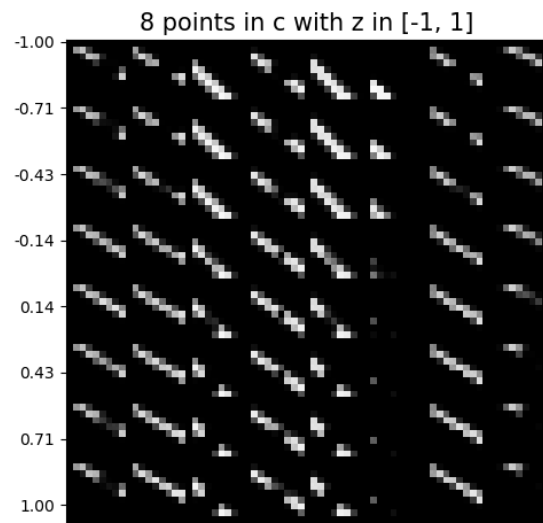


Figure 7: Points in  $C$  while varying  $z$ . The perspective defined by  $c$  remains fixed while  $z$  varies the line break perturbation.